

# The resistivity image of the Muráň fault zone (Central Western Carpathians) obtained by electrical resistivity tomography

RENÉ PUTIŠKA<sup>1</sup>✉, IVAN DOSTÁL<sup>1</sup>, ANDREJ MOJZEŠ<sup>1</sup>, VOJTECH GAJDOS<sup>1</sup>, KAMIL ROZIMANT<sup>1</sup>  
and RASTISLAV VOJTKO<sup>2</sup>

<sup>1</sup>Department of Applied and Environmental Geophysics, Faculty of Natural Sciences, Comenius University, Mlynská dolina G,  
842 15 Bratislava, Slovak Republic; ✉putiska@fns.uniba.sk

<sup>2</sup>Department of Geology and Paleontology, Faculty of Natural Sciences, Comenius University, Mlynská dolina G, 842 15 Bratislava,  
Slovak Republic

(Manuscript received June 9, 2011; accepted in revised form September 30, 2011)

**Abstract:** The paper describes the application of geophysical prospecting techniques for estimation of the fault's inclination. The field survey was carried out across the Muráň fault structure in the Slovenské rudohorie Mts (central Slovakia). Three different geophysical methods were used to map the fault zone: Electrical Resistivity Tomography (ERT), induced polarization (IP) and radon emanometry. All these methods have been used to locate the fault zone area, but the principal aims of this research are to test the efficiency of the 2D ERT technique to recognize the geometrical characterization of the fault and to improve our tectonic knowledge of the investigated area. For the synthetic cases, three geometric contexts were modelled at 60, 90 and 120 degrees and computed with the  $l_2$  norm inversion method, the  $l_1$  norm with standard horizontal and vertical roughness filter and the  $l_1$  norm with diagonal roughness filter. In the second phase this geophysical methodology was applied to fieldwork data. Our results confirm that the ERT technique is a valuable tool to image the fault zone and to characterize the general geometry, but also the importance of setting up the right inversion parameters. The main contribution of the geophysical investigations in this case was the determination of the location and confirmation of the inclination of the Muráň fault. The result of this study is the ability to make a visual estimation of the direction and dip of the fault. Pursuant to this work the dipole-dipole electrode configuration produces the best resolution, particularly for the location of vertical and dipping structures. The advantage of this array is that it shows the ability to assess the trend of the dip and therefore it can be strongly recommended. The result is also a case study of a small scale tectonic survey involving geophysical methods.

**Key words:** Central Western Carpathians, Muráň fault zone, geophysical prospecting, electrical resistivity tomography, induced polarization, radon emanometry.

## Introduction

The study area is located in the central part of the Central Western Carpathian Mountain Belt (the Slovenské rudohorie Mts, Fig. 1). The area consists of the Carnian Wetterstein limestone of the Muráň Nappe belonging to the Silicic Unit (cf. Kozur & Mock 1973; Mello 1979), Lower Paleozoic gneisses of the Southern Veporic Unit (cf. Bystrický 1959; Klinec 1976; Hovorka et al. 1987) and Quaternary consolidated breccias (cf. Ložek 1960).

The main goal of this paper is to present a study that contributes to the determination of the exact position, depth continuation and inclination of the Muráň fault structure. In the study of fault system geometry, a common procedure is to make use of information from stratigraphic, structural and geomorphological studies. This information could be obtained from drilling and exploration boreholes. However, these methods are expensive and time consuming, which prevents their use on a large scale. Moreover, these types of data are spatially limited. In contrast, geophysical measurements can provide a less expensive way to improve our knowledge. In many cases, geophysical prospecting tech-

niques can provide complementary data that enable geological correlation, even in parts where there are no data from boreholes. In this area an outcrop has been found, where it is possible to see the contact between Mesozoic sequence (Wetterstein limestone and dolomite) and Lower Paleozoic crystalline basement (gneisses) Fig. 2. This place was used as electrical resistivity tomography (ERT) reference profile. The result of the reference measurement was used as the entry parameter to prepare models for the forward modelling program Res2Dmod (Loke 2002). Three different geophysical methods were used to map the fault zone. Resistivity survey (ERT) was complemented by the measurement of IP (induced polarization) and radon gas concentration in soil air (radon emanometry). The principal aims of this research are to test the efficiency of the 2D ERT technique with the different arrays to recognize the geometrical characterization of the fault using smooth inversion methods and block inversion methods. These two methods were compared by Olayinka & Yaramancı (2000) and Loke et al. (2003), who demonstrated the characteristics, advantages and drawbacks of both methods. They concluded that in cases where the resistivity contrast is gradual, smooth inversion is more suitable, whilst

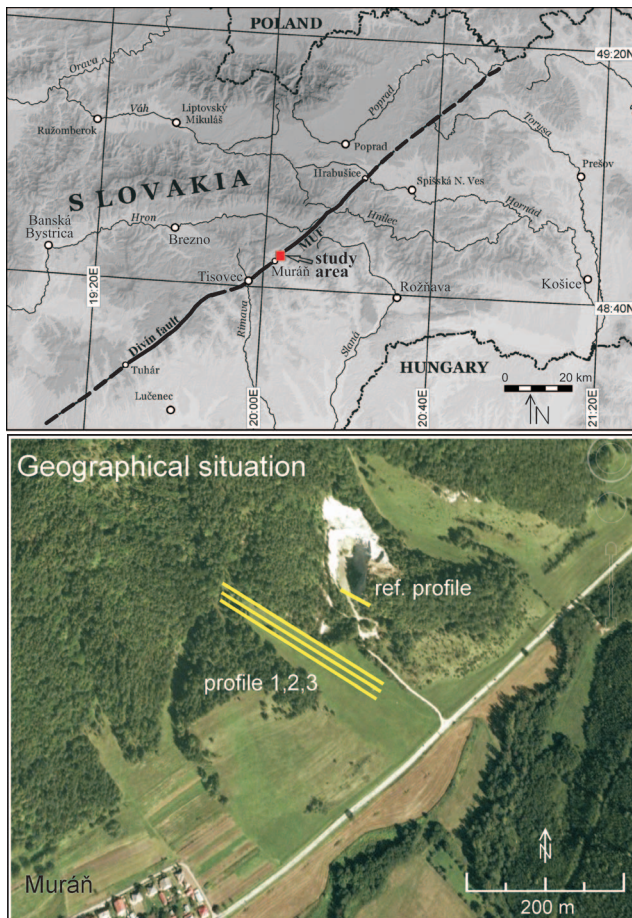


**Fig. 1.** Location map with geological situation of survey site in the Muráň fault area (according to Klinec 1976, modified).

when there is a sharp variation in resistivity contrast, block inversion is preferable. Checking and changing some mathematical parameters, such as damping factors, ratio of thickness of the first layer, diagonal filter and the smoothness matrix, can also be performed (Cardarelli & Fischanger 2006). Furthermore, modifying the inversion results by changing the starting model appears to be the best way to obtain valid physical results from the inversion. The results of measurement are also affected by electrode arrays (Mendoza & Dahlin 2008). The resolution and penetration depth of arrays also depend on the geological models (electrical properties, anomaly body geometry) and the noise contamination levels, all of which may be efficiently simulated by numerical methods (Dahlin & Zhou 2004).

### Geological setting

The Muráň fault is the most distinctive disjunctive structure in the Western Carpathians which is evident by its geological structure and terrain morphology. The Muráň fault was first described by Zoubek (1935), according to the village of Muráň. This fault is considered to be predominantly a strike-slip fault with dominant left-lateral movement (e.g. Plašienka 1983; Pospíšil et al. 1989; Marko 1993; Vojtko 2003; Vojtko

et al. 2011). The NE-SW trending Muráň fault forms a very straight discontinuity, which separates carbonates on the north-western side from the crystalline basement on the south-eastern side (Fig. 1). The Muráň fault represents a strongly deformed zone and the host rocks are intensively mylonitized.

The north-western block is composed of the Wetterstein limestone of the Muráň Nappe which belongs to the Silicic Unit. In the study area the Wetterstein limestone is dolomitized or changed to dolomite. In this dolomite the limestone forms small irregular bodies, mainly lenses or layers. The dolomite is of light grey to grey colour, and has a grained or massive fabric. The bedding is visible mainly as alternating dark and light thin beds. The thickness of the Wetterstein Formation is from 75 to 375 m; about 250 m is the average thickness (Bystrický 1959; Vojtko 2000).

The south-eastern block consists of Lower Paleozoic metamorphites of the Southern Veporic Unit (cf. Hovorka et al. 1987; Vozárová & Vozár 1988; Hók & Vojtko 2011). The main lithotypes of this crystalline basement are middle-grained gneisses over the fine-grained ones occasionally with layers of amphibolites (Klinec 1976; Hovorka et al. 1987; Bezák et al. 2009).

The upper stratum in the study area consists of breccia. The Pleistocene Muráň breccias are composed of carbonate detritus cemented by calcareous sinter. The cement is often compact and occasionally porous. The bedding of these breccias is parallel to the slope (Ložek 1960).

### Synthetic study

The reference profile was measured very closely to the uncovered subvertical contact between the Wetterstein Formation and the crystalline basement (gneisses) (Fig. 2). The purpose of the reference ERT measurement was to obtain real values of resistivity to prepare synthetic models fitted to real geological formation.

In this case, the result of the reference measurement was used to prepare input data for the numerical model to simulate the geological situation along the synthetic model. The synthetic data are computed using the forward modelling program Res2Dmod (Loke 2002). The synthetic models represent the tree geometries of the contact of two environments (a vertical 90° and a dipping 60° and 120°) and they represent a simplified geological and structural sketch along the investigated profile. Synthetic data sets were generated for dipole-dipole, pole-dipole, Wenner alpha and Schlumberger arrays. The electrode spacing was 5.5 m for simple comparison with real data.

### Field study

The task of the field study was to define the exact position and inclination of the Muráň fault. The inversion procedure and the new knowledge from the modelling presented above was applied to the field study.

The study profiles were located transversely on the Muráň fault, close to the village of Muráň (Fig. 1) and the measure-

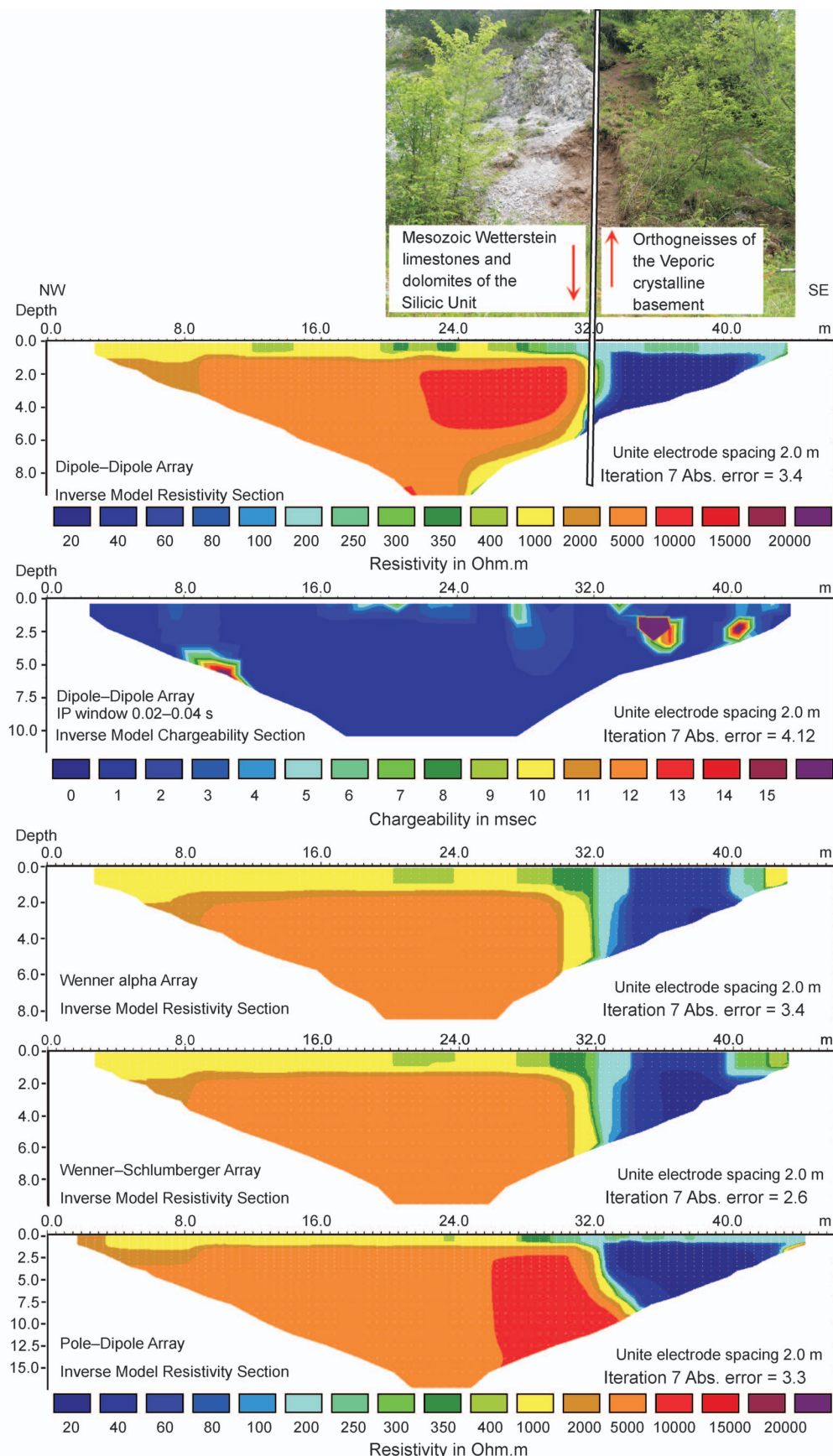
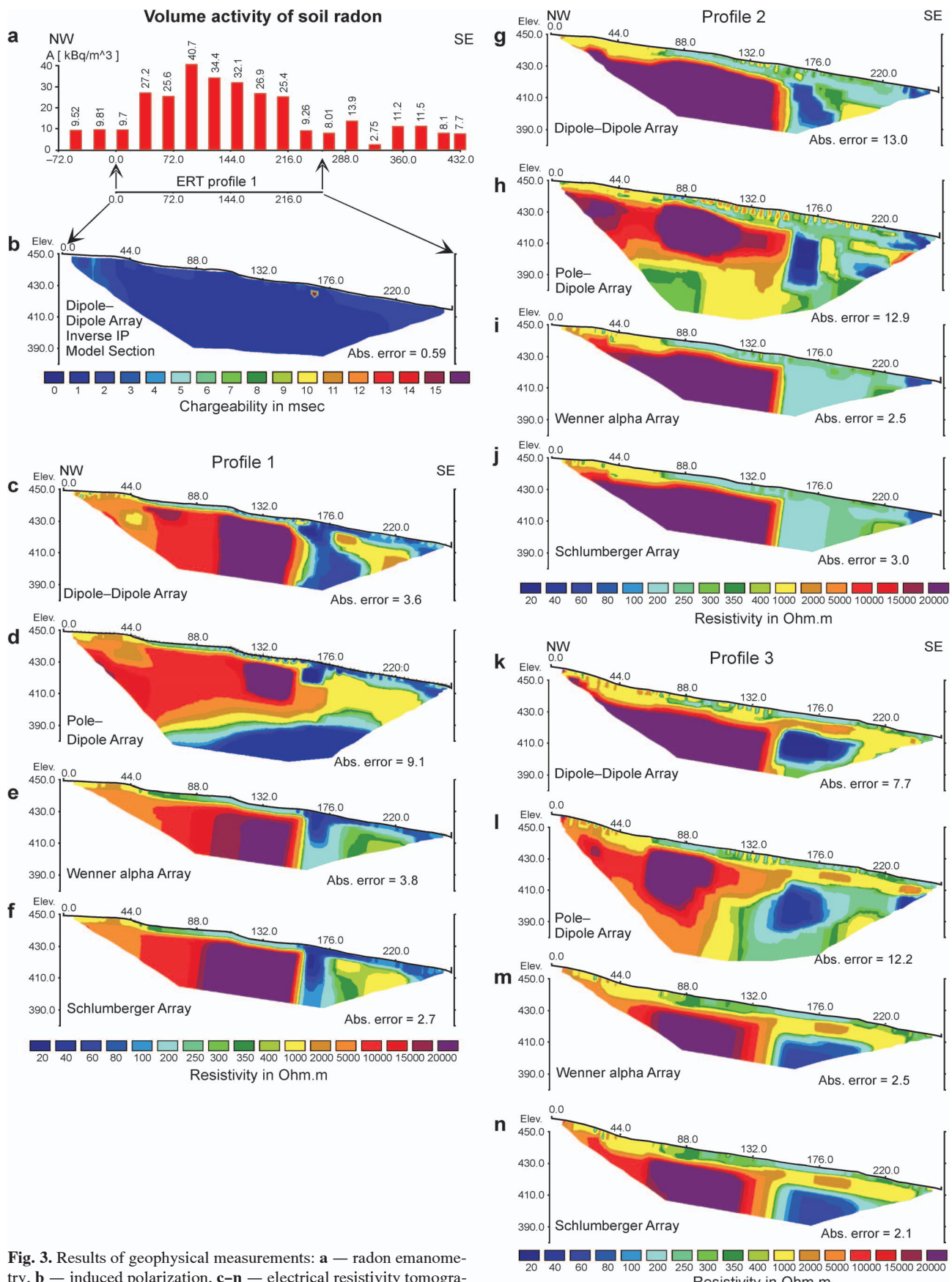


Fig. 2. Results of reference geophysical measurements — Electrical resistivity tomography and induced polarization (horizontal scale in meters).



**Fig. 3.** Results of geophysical measurements: **a** — radon emanometry, **b** — induced polarization, **c-n** — electrical resistivity tomography (horizontal scale in meters).

ment was performed with four different arrays: dipole-dipole (DD) (Fig. 3c,g,k), pole-dipole (PD) (Fig. 3d,h,l), Wenner alpha (WA) (Fig. 3e,i,m), Schlumberger (SCH) (Fig. 3f,j,n) to enable the comparison with synthetic models. Profile 1 was complemented by IP (Fig. 3b) and radon emanometry (Fig. 3a). The IP result shows that this method was not very successful in this particular case.

Three 2D electrical resistivity tomography lines "Profiles 1, 2 and 3" (Fig. 3) were collected using ARES instrument (GF Instruments, CZ). The ERT profiles were oriented roughly perpendicular to the investigated fault trace and all three profiles had the same configuration. The distance between the profiles was 11 m. For localization and elevation of the profile, the GPS system Trimble, Pathfinder ProXH was used.

Radon emanometry is an atmogeochemical survey method based on the measurement of alpha activity of soil air samples taken from the same depth of rock weathering cover. The alpha activity is a result of the alpha disintegration process of nuclei of radon isotope  $^{222}\text{Rn}$  and its daughter products. As the parent radium isotope  $^{226}\text{Ra}$  commonly occurs in rock fabric and  $^{222}\text{Rn}$  is a gaseous element, the fault system is a very appropriate way for upward moving not only for radon but also for other Earth gases. Thus the volume activity ( $\text{kBq} \cdot \text{m}^{-3}$ ) of soil radon gas measurements along the profile crossing the assumed fault zone could contribute considerably to its more exact characterization (Grunorád & Mazáč 1994; Giannamano et al. 2009). The radon measurements were performed with the portable radon detector LUK-3R (SMM, CZ) with sampling from the same depth of about 0.8 m.

Figure 3 shows the result of the field-work, where the north-western part is characterized by high values of interpreted resistivity, while the resistivity in the south-eastern part is less than  $100 \Omega\text{m}$ . A fault, which can be clearly seen in the image, separates both types of structures. The inversion results show, that if there is a good resistance contrast between two environments, it is easy to determine the contact of these two environments using the electrical resistivity tomography.

As mentioned above, the measurement was performed with four different arrays (DD, WA, SCH, and PD). The DD may provide higher image resolution than PD, WA and SCH. The WA and SCH arrays show sharp vertical contact for all three profiles (Fig. 3e,f,i,j,m,n), but after the comparison with synthetic models it is possible to see that these two arrays show a sharp, almost a  $90^\circ$ , vertical contact also for the dip of  $60^\circ$ , and  $120^\circ$ . The WA and SCH configurations show a perfect resistivity contact but the resolution for dipping structure is low.

The results of the PD arrays (Fig. 3d,h,l) have the highest root

mean square (RMS) error for all profiles. During the modelling the PD array has shown capacity to recognize the dip of the fault, but the result of the fieldwork was affected by a high noise level in the deepest part. The PD array has the best depth penetration and the result shows the ability to locate vertical or dipping structures but with a lower image resolution.

The imaging resolution of the DD array (Fig. 3c,g,k) is best for all three profiles and is much better than in case of the other arrays, particularly for the location of vertical and dipping structures. The result of the DD array was chosen for 3D modelling. The data from P1, P2 and P3 profiles were collated in RES3DINV software. The  $l_1$  norm with  $xy$  and  $yz$  diagonal roughness filter was used for forward modelling calculation. The result was used for 3D visualization (Fig. 4a), where the contact of the two lithological blocks and the dip of the fault, which is almost  $90^\circ$  toward the south-east, can be clearly seen. The geological map shows the exact contact of the Veporic crystalline basement and the Mesozoic sequence of the Silicic Unit from the geophysical survey (Fig. 4b).

The location of the fault zone is also visible on the profile curve of the radon volume activity in the soil air (Fig. 3a). The fault zone seems to be much wider than it appears from the ERT measurements. This is logical evidence of the higher looseness of rock material around the fault zone on both sides — over weathered Mesozoic carbonates as well as over Lower Paleozoic gneisses, which resulted in higher gas permeability and therefore in higher radon gas flux from the deeper parts.

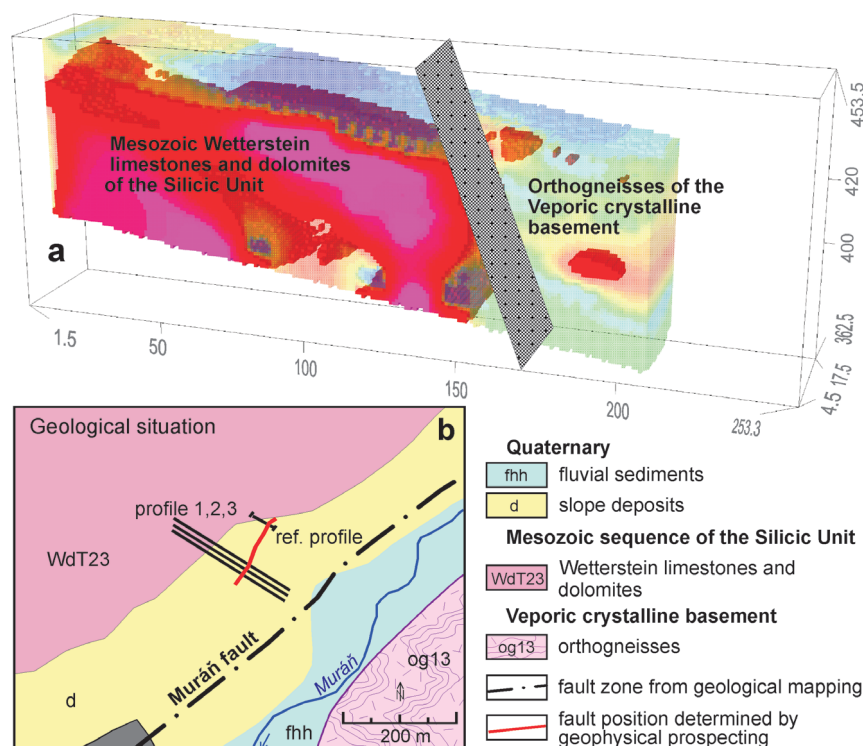


**Fig. 4.** 3D results of electrical resistivity tomography with the direction of the fault and map of the geological situation show the exact contact of the Veporic crystalline basement and the Mesozoic sequence of the Silicic Unit from the geophysical survey.

## Conclusions

On the basis of the former geological and geophysical studies the Muráň fault can be identified as a deep-seated regional crustal fault. The analysis of the total Bouguer anomalies and different transformed gravity maps indicates that the fault is characterized by significant gravity gradient (e.g. Fusán et al. 1971, 1987). On the set of new gravity maps consisting of total Bouguer and regional gravity anomalies from the Carpathian-Pannonian Basin region the Muráň fault can also be observed approximately from Ľubľana to Lublin (Bielik et al. 2006; Bielik & Wybraniec 2007; Bielik & Mikuška 2007; Alasonati Tašárová et al. 2008, 2009). Taking into account the results published by Vozár et al. (2010) in the Western Carpathians the evolution of the Muráň fault could also be related to the evolution of another regional crustal fault, which is known as Diósjenő Line.

The main contribution of the geophysical investigations in this case was the determination of the location and confirmation of the inclination of a small part of the Muráň fault (Fig. 4). The result of geophysical prospecting is showing the exact contact of the Veporic crystalline basement and the Mesozoic sequence of the Silicic which is approximately 250 m north-west from the geological mapping (Fig. 4b).

The result of this study is the ability to make a visual estimation for the direction and the dip of the fault. In this case calculated inversion models from synthetic data have been compared with calculated inversion models using real data measurement. The data have been calculated by the  $l_1$  norm with diagonal roughness filter. The 2D inversion result of the reference profile and resistivity profile correlated with synthetic models.

In the context of this work, the DD electrode configuration produces the best resolution, particularly for the location of vertical and dipping structures. The advantage of this array is that it shows the ability to assess the trend of the dip and therefore it can be strongly recommended.

**Acknowledgments:** The authors are grateful to the the Slovak Research and Development Agency APVV (Grant Nos. APVV-0194-10, APVV-0158-06) and the Slovak Grant Agency VEGA (Grant Nos. 1/0095/12, 2/0067/12, 1/0747/11, 1/0468/10) for the support of their research.

## References

Alasonati Tašárová Z., Bielik M. & Götze H.J. 2008: Stripped image of the gravity field of the Carpathian-Pannonian region based on the combined interpretation of the CELEBRATION 2000 data. *Geol. Carpathica* 59, 3, 199–209.

Alasonati-Tašárová Z., Afonso J.C., Bielik M., Götze H.J. & Hók J. 2009: The lithospheric structure of the Western Carpathian-Pannonian Basin region based on the CELEBRATION 2000 seismic experiment and gravity modelling. *Tectonophysics* 475, 454–469.

Bezák V., Biely A., Broska I., Bóna J., Buček S., Elečko M., Filo I., Fordinál K., Gazdačko Ľ., Grecula P., Hraško Ľ., Ivanička J., Jacko S. (Sr.), Jacko S. (Jr.), Janočko J., Kaličiak M., Kobulský J., Kohút M., Konečný V., Kováčik M. (Bratislava), Kováčik M. (Košice), Lexa J., Madarás J., Maglay J., Mello J., Nagy A., Németh Z., Olšavský M., Plašienka D., Polák M., Potfaj M., Pristaš J., Siman P., Šimon L., Teták F., Vozárová A., Vozár J. & Žec B. 2009: Explanation text to General Geological Map of Slovak Republic (1:200,000). *ŠGÚDŠ*, Bratislava, 1–534.

Bielik M. & Mikuška J. (Eds.) 2007: Transformed maps of total bouguer anomalies of Austria, Czech Republic, Hungary, Poland and Slovak Republic. *MS Faculty of Natural Sciences Comenius University*, Bratislava, *EQUIS*, s.r.o., Bratislava.

Bielik M. & Wybraniec S. (Eds.) 2007: Transformed maps of total bouguer anomalies of Austria, Czech Republic, Hungary, Poland and Slovak Republic. *MS Faculty of Natural Sciences Comenius University*, Bratislava, *EQUIS*, s.r.o., Bratislava.

Bielik M., Kloska K., Meurers B., Švancara J., Wybraniec S. & CELEBRATION 2000 Potential Field Working Group 2006: Gravity anomaly map of the CELEBRATION 2000 region. *Geol. Carpathica* 57, 3, 145–156.

Bystríký J. 1959: A contribution to the stratigraphy of the Muráň Mesozoic. *Geol. Práce, Zoš.* 56, 1–53.

Cardarelli E. & Fischanger F. 2006: 2D data modelling by electrical resistivity tomography for complex subsurface geology. *Geophys. Prospect.* 54, 2, 121–133.

Dahlin T. & Zhou B. 2004: A numerical comparison of 2D resistivity imaging with 10 electrode arrays. *Geophys. Prospect.* 52, 5, 379–398.

Fusán O., Ibrmajer J., Plančár J., Slávik J. & Smíšek 1971: Geological structure of the basement of the covered parts of southern part of Inner West Carpathians. *Zborn. Geol. Vied, rad ZK* 15, 1–173 (in Slovak).

Fusán O., Biely A., Ibrmajer J., Plančár J. & Rozložník L. 1987: Basement of the Tertiary of the Inner West Carpathians. *GÚDŠ*, Bratislava, 1–123 (in Slovak).

Giammanco S., Immé G., Mangano G., Morelli D. & Neri M. 2009: Comparison between different methodologies for detecting radon in soil along an active fault: The case of the Pernicana fault system, Mt. Etna (Italy). *Applied Radiation and Isotopes* 67, 1, 178–185.

Gruntorád J. & Mazáč O. 1994: Impact of subtle dynamic geofactors on environment. *Acta Universitatis Carolinae Environmentalica* 8, 3–53.

Hovorka D., Dávidová Š., Fejdi P., Gregorová J., Hatář J., Kátlovský V., Pramuka S. & Spišiak J. 1987: The Muráň Gneisses — the Kohút crystalline Complex, the Western Carpathians. *Acta Geol. Geogr. Univ. Comenianae, Geol.* 42, 5–101.

Hók J. & Vojtko R. 2011: Continuation of the Pohorelá line in pre-Cenozoic basement of the Central Slovakia Volcanic Field (Western Carpathians). *Acta Geol. Slovaca* 3, 1, 13–19 (in Slovak with English summary).

Klinec A. 1976: Geological map of Slovenské Rudohorie and Nízke Tatry Mts. *GÚDŠ*, Bratislava (in Slovak).

Kozur H. & Mock R. 1973: Zum Alter und zur tektonischen Stellung der Meliata-Serie des Slovakischen Karstes. *Geol. Zbor. Geol. Carpath.* 24, 365–374.

Loke M.H. 2002: Tutorial. Res2dmod ver. 3.01, Rapid 2D resistivity forward modelling using the finite-difference and finite-element methods. *Geotomo Software*, Malaysia.

Loke M.H., Acworth I. & Dahlin T. 2003: A comparison of smooth and blocky inversion methods in 2D electrical imaging surveys. *Explor. Geophys.* 34, 3, 182–187.

Ložek V. 1960: Muráň breccias. *Věstník ÚÚG*, Praha, 25 (in Czech).

Marko F. 1993: Kinematics of Muráň fault between Hrabašice and Tuhár village. In: Rakús M. & Vozár J. (Eds.): Geodynamic model and deep structure of the Western Carpathian. *Conf. Symp. Sem.*, *ŠGÚDŠ*, Bratislava, 269–277.

Mello J. 1979: Belong the higher Subtatic nappes and the Silica nappe to the Gemeric unit? *Miner. Slovaca* 11, 3, 279–281 (in Slovak).

Mendoza J.A. & Dahlin T. 2008: Resistivity imaging in steep and weathered terrains. *Near Surface Geophysics* 6, 2, 105–112.

Olayinka A.I. & Yaramanci U. 2000: Assessment of the reliability of 2D inversion of apparent resistivity data. *Geophys. Prospect.* 48, 2, 293–316.

Plašienka D. 1983: Geological structure of the Tuhár Mesozoic (Central Slovakia). *Miner. Slovaca* 15, 1, 49–58.

Pospíšil L., Bezák V., Nemčok J., Feranec J., Vass D. & Obernauer D. 1989: The Muráň tectonic system as example of horizontal displacement in the West Carpathians. *Miner. Slovaca* 21, 4, 305–322.

Vojtko R. 2000: Are there tectonic unit derived from the Meliata-Hallstatt trough incorporated to the tectonic structure of the Tisovec Karst? (Muráň karstic plateau, Slovakia). *Slovak Geol. Mag.* 6, 4, 335–346.

Vojtko R. 2003: Structural analysis of faults and geodynamic evolution of the central part of the Slovenské Rudohorie Mts. *Manuscript, PhD Thesis, Comenius University, Bratislava*, 1–91 (in Slovak).

Vojtko R., Marko F., Preusser F., Madarás J. & Kováčová M. 2011: Late Quaternary fault activity in the Western Carpathians: evidence from the Vikartovce Fault (Slovakia). *Geol. Carpathica* 62, 6, 563–574.

Vozár J., Ebner F., Vozárová A., Haas J., Kovács S., Sudar M., Bielik M. & Péró Cs. (Eds.) 2010: Variscan and Alpine terranes of the Circum-Pannonian region. *Slovak Acad. Sci., Geol. Inst., Bratislava*, 7–233.

Vozárová A. & Vozár J. 1988: Late Paleozoic in West Carpathians. *GÚDŠ*, Bratislava, 7–314.

Zoubek V. 1935: Tectonics of the Upper Hron valley and its relation to the mineral water springs. *Věst. SGÚ ČSR*, Praha 11, 5, 85–115 (in Czech).